Accurate Calculation of Eye Diagrams and Error Rates in Long-Haul Transmission Systems

R. Holzlöhner,[1] **C. R. Menyuk,**[1,2] **V. S. Grigoryan,**[1] **and W. L. Kath**[3,1]

[1] *Department of Computer Science and Electrical Engineering, University of Maryland Baltimore County, TRC 201 B, 1000 Hilltop Circle, Baltimore, MD 21250*
tel: 410-455-3318, fax: 410-455-6500, email: holzloehner@umbc.edu
http://www.photonics.umbc.edu/

[2] *Laboratory for Telecommunications Sciences, c/o USARL, Bldg. 601, Rm. 131, 2800 Powder Mill Road, Adelphi, MD 20783-1197*

[3] *Department of Engineering Sciences and Applied Mathematics, Northwestern University, 2145 Sheridan Road, Evanston, IL 60208-3125*

Abstract: We found the distribution of phase and timing jitter in a DMS system to be Gaussian-distributed. After their removal, the residual noise Fourier components obey a multivariate-Gaussian distribution, allowing us to accurately calculate eye diagrams and error rates.

OCIS codes: (060.0060) Fiber optics communications; (270.2500) Fluctuations, relaxations, and noise

1 Introduction

In current optical fiber communication systems, amplifier spontaneous emission (ASE) noise sets the lower limit on the allowed system power [1], [2]. At the receiver, ASE noise leads to amplitude and timing jitter and deteriorates the bit error rate (BER). The noise spectrum is white over the spectral width of one channel. However, due to the nonlinearity of the optical fibers leading to cross-phase modulation and four-wave mixing, the noise interacts with the signal in a complex way that usually increases the signal degradation. The traditional computation of the probability distribution function (pdf) of the electrical signal in the receiver, based on Monte-Carlo simulations, only works for a limited range of BERs beyond which the BER has to be extrapolated [3]. Extrapolation methods to date assume that the noise power is Gaussian-distributed. This assumption often yields good results in comparison of theory and experiment [4], but it is not always reliable. First, it assumes that the nonlinear beating of the noise with itself during the optical transmission is negligible, i.e., the system is linearizable. Second, it assumes that the actual distribution function for the marks and spaces, which would both be chi-square distributions [5], can be replaced by Gaussians. In this contribution, we numerically study a single-channel dispersion-managed soliton (DMS) system for lengths up to 24,000 km, and we show that once the phase and timing jitter are properly removed, the residual Fourier components all obey a multivariate Gaussian distribution. Thus, a linearization approach in which one neglects the nonlinear interaction of the noise with itself during transmission is valid to within the limits of numerical accuracy and allows us to accurately calculate the eye diagrams and error values. (Of course, the quadratic nonlinearity in the receiver must be retained in the calculation.) We focused on this system because it is well-characterized experimentally [4] and it is highly nonlinear and thus represents a stringent test of our approach. We thus believe that this approach will be of use in a wide variety of systems, although its full scope remains to be determined. We are extending previous work in which we showed that the linearization is valid when calculating the amplitude and timing jitters for several different formats [6].

We conducted Monte-Carlo simulations of a single-channel DMS system over 24,000 km similar to [4]. We investigated the pdfs of both the phase and timing jitters. We verified that the timing jitter is Gaussian and that the phase jitter is distributed like a Jacobi θ-function, which is the periodic analog to a Gaussian [7]. When the phase and timing jitter is removed from the received signal with the help of a simple analytical transform, we find that the residual noise components are Gaussian-distributed. This in turn allows us to obtain the multivariate Gaussian distribution of the noise Fourier coefficients b_i, based on the covariance matrix $K_{ij} = \langle b_i b_j^* \rangle$. We may then calculate the pdf for the spaces and the marks, taking into account the timing jitter. The phase jitter makes no contribution. This procedure is a generalization of [8], as the diagonal elements of K are not equal.

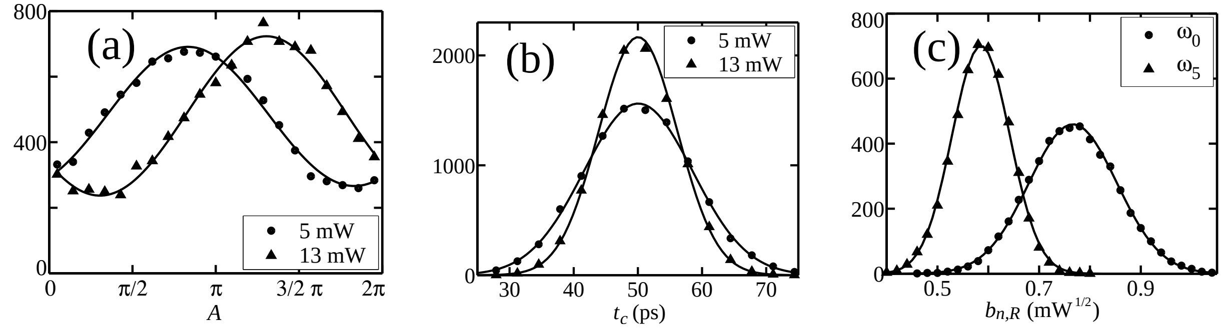

Fig. 1. (a) Histogram of A and (b) histogram of $t_c = -B/\Delta\omega$ for two different signal peak powers $P_p =$ 5 mW and $P_p = 13$ mW. (c) Histogram of the two real Fourier coefficients $b_{0,R}$ and $b_{5,R}$ at $\omega_0 = 0$ and $\omega_5 = 2\pi \times 25$ GHz, respectively, after the linear part of the phase is removed ($P_p = 5$ mW). The solid lines are fits of the Jacobi θ-function in (a) and Gaussians in (b) and (c). The simulation consists of 10,000 Monte-Carlo runs.

2 Theory and Results

We conducted Monte-Carlo simulations of a DMS system, transmitting a single soliton. We consider the received signal in the frequency domain $\widetilde{u}(\omega) = \widetilde{u}_0(\omega) + \delta\widetilde{u}(\omega)$, where $\widetilde{u}_0$ is the signal average over all noise realizations and $\delta\widetilde{u}$ is the total noise at the receiver. For single pulse transmission, $\widetilde{u}$ can be decomposed as

$$\begin{aligned} u &= u_0 + \delta u = u_0 \exp\big[i(\alpha + \beta\omega)\big] + r, && \text{(1a)} \\ \delta u &\approx i\alpha u_0 + i\beta\omega u_0 + r, && \text{(1b)} \end{aligned}$$

where α and β are real numbers. The part of the noise that is responsible for a phase shift is proportional to iu_0, while the component $i\beta\omega u_0$ leads to timing jitter. For each noise realization of the Monte-Carlo simulation, we fit a linear function to the phase of $\widetilde{u}(\omega)$ using a least-squares criterion,

$$I = \min_{A,B} \int_{-\infty}^{\infty} |u|^2 \left[\arctan \frac{\widetilde{u}_I}{\widetilde{u}_R} - A - B\omega\right]^2 \mathrm{d}\omega, \tag{2}$$

where $\widetilde{u} = \widetilde{u}_R + i\,\widetilde{u}_I$. We found the linear phase assumption is good as long as the receiver is placed at the chirp-free maximum compression point of the dispersion map. The fit then yields the estimates $\alpha \approx A$ and $\beta \approx B$ from which we obtain $\widetilde{u}_{\mathrm{rem}} = \widetilde{u}\exp[-i(A + B\omega)] \approx \widetilde{u}_0 + r\exp[-i(A + B\omega)]$. The Fourier series expansion of $u_{\mathrm{rem}}(t)$ is $u_{\mathrm{rem}}(t) = \sum_{n=-N/2}^{(N/2)-1} b_n \exp(i\omega_n t)$, $\omega_n = 2\pi n/T$, with the N complex coefficients $b_n = b_{n,R} + i\,b_{n,I}$, where T is the period. We tested the hypothesis that the central time of the pulses, $t_c = -B/\Delta\omega$, as well as that $b_{n,R}$ and $b_{n,I}$ are Gaussian-distributed, where $\Delta\omega = \omega_{k+1} - \omega_k = 2\pi/T$. We fit the distribution of A to a Jacobi θ-function [7] with

$$\theta_\psi(\mu, \sigma^2, 2\pi) = \sum_{k=-\infty}^{\infty} \mathcal{N}_{\psi+2\pi k}(\mu, \sigma^2), \tag{3}$$

where $\mathcal{N}_x(\mu, \sigma^2)$ is a Gaussian (normal) distribution of mean μ and variance σ^2 taken at x. The θ-function is the natural choice for the phase fit since A is only determined modulo 2π.

Our simulated transmission line consists of 225 dispersion maps of length 107 km each [4]. Each map contains a normal span of 4×25 km and dispersion $D_n = -1.03$ ps/nm-km and an anomalous span of 6.7 km and $D_a = 16.7$ ps/nm-km. The average dispersion is $D_{\mathrm{av}} = 0.08$ ps/nm-km. The fiber loss is compensated by five EDFAs and there is a 2.8 nm optical bandpass filter in each map to reduce the amount of noise. The spontaneous emission factor is $n_{\mathrm{sp}} = 1.3$. The signal has a Gaussian shape with a minimum FWHM duration of about 9 ps and is launched and received in the midpoint of the anomalous span.

Figures 1 (a) and (b) show histograms of A and $t_c = -B/\Delta\omega$ for two different signal peak powers P_p. Each simulation consists of 10,000 Monte-Carlo runs. The linear phase fit of Eq. (2) is very good even at the large transmission distance of 24,000 km. Pulses are launched at $t_c = 50$ ps.

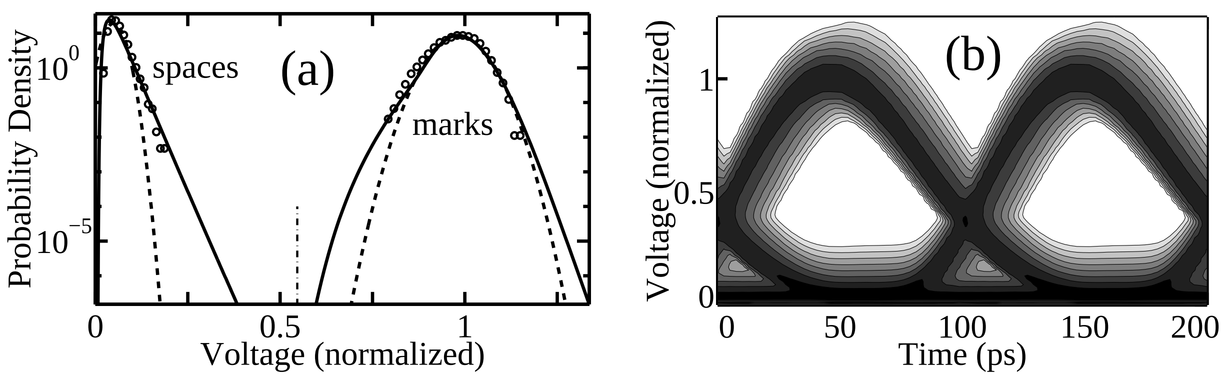

Fig. 2. (a) Analytical pdf of the noise voltage after square-law detection and an 8.6 GHz Bessel filter. The solid lines are the pdfs taken at $t = 50$ ps for the marks (1's) and between pulses for the spaces (0's); the dashed lines are Gaussian fits. The pdfs include the effect of the timing jitter (the standard deviation of t_c). Note that the Gaussian fits are good over about two orders of magnitude, but deviate strongly at low probabilities. The pdf of the marks is dominated by timing jitter at low voltages, leading to a visible bump. The exponential decay of the pdf of the spaces results from the quadratic noise term in the receiver [8]. The circles are results from the Monte-Carlo simulation and can be thought of as a slice through an electrical eye diagram. Particularly for the spaces, the agreement with the analytical pdf is much better than for the Gaussian fit. (b) A contour plot of the pdfs mimicking an eye diagram. The logarithm of the pdf is displayed as different shades of gray. To obtain a more readable diagram, we only plot probabilities in the range $[10^{-4}, 10^{1}]$, while our approach allows us to find the probability density for any voltage, thereby enabling us to calculate exact BERs. The optimal decision level in (a) lies at 0.546 (see the dash-dotted line) and yields a BER of 5.34×10^{-13}. From the Gaussian fits, we obtain a Q-factor of 13.5 implying a BER of 10^{-41} instead.

Figure 1 (c) shows histograms of $b_{0,R}$ and $b_{5,R}$ at the angular frequencies $\omega_0 = 0$ and $\omega_5 = 2\pi \times 25$ GHz, respectively. The simulated data agree very well with the Gaussian fit. The way we removed the linear part of the signal phase causes the imaginary parts of the b_n to be close to zero; so, they are not shown here. Figure 2 (a) shows the pdf of the voltage after the electrical receiver, calculated from the covariance matrix K, which has a generalized chi-square distribution [5, 8]. The effect of the timing jitter is analytically included in the calculation of the pdfs. Figure 2 (b) shows the corresponding eye diagram.

3 Conclusion

We performed Monte-Carlo simulations over 24,000 km of a DMS system similar to [4] and investigated the distribution of the phase and timing jitters. We find the timing jitter to be Gaussian-distributed, while the phase jitter obeys a Jacobi θ-distribution, which is the periodic analog of a Gaussian distribution. We also examined the distribution of the Fourier coefficients of the received signal after the phase and timing offsets are removed from each signal. These components obey a multivariate Gaussian distribution. Using these results, we can accurately calculate the eye diagrams and the bit error rates. In the future, we will determine the applicability of this approach to other systems.

References

1. J. P. Gordon and H. A. Haus, "Random walk of coherently amplified solitons in optical fiber transmission," Opt. Lett. **11,** 665–667 (1986).
2. H. A. Haus, "Quantum noise in solitonlike repeater systems," J. Opt. Soc. Amer. B **8,** 1122–1126 (1991).
3. N. S. Bergano, F. W. Kerfoot, and C. R. Davidson, "Margin measurements in optical amplifier systems," IEEE Photon. Technol. Lett. **5,** 304–306 (1993).
4. R.-M. Mu, V. S. Grigoryan, C. R. Menyuk, G. M. Carter, and J. M. Jacob, "Comparison of theory and experiment for dispersion-managed solitons in a recirculating fiber loop," IEEE J. Sel. Topics Quant. Electronics **6,** 248–257 (2000).
5. J. G. Proakis, *Digital Communications* (McGraw-Hill, New York, 1995).
6. V. S. Grigoryan, C. R. Menyuk, and R.-M. Mu, "Calculation of timing and amplitude jitter in dispersion-managed optical fiber communications using linearization," J. Lightwave Technol. **17,** 1347–1356 (1999).
7. M. Abramowitz and I. A. Stegun, *Handbook of Mathematical Functions* (Dover, 1965).
8. D. Marcuse, "Derivation of analytical expressions for the bit-error probability in lightwave systems with optical amplifiers," J. Lightwave Technol. **8,** 1816–1823 (1990).